ORIGINAL ARTICLE

Diabetic Retinal Neurodegeneration Is Associated With Mitochondrial Oxidative Stress and Is Improved by an Angiotensin Receptor Blocker in a Model Combining Hypertension and Diabetes

Kamila C. Silva, Mariana A.B. Rosales, Subrata K. Biswas, Jose B. Lopes de Faria, and Jacqueline M. Lopes de Faria

OBJECTIVE—Diabetic retinopathy displays the features of a neurodegenerative disease. Oxidative stress is involved in the pathogenesis of diabetic retinopathy. This investigation sought to determine whether hypertension exacerbates the oxidative stress, neurodegeneration, and mitochondrial dysfunction that exists in diabetic retinopathy and whether these changes could be minimized by the angiotensin II type 1 (AT_1) receptor blocker (ARB) losartan.

RESEARCH DESIGN AND METHODS—Diabetes was induced in spontaneously hypertensive rats (SHRs) and normotensive Wistar-Kyoto (WKY) rats. The diabetic SHRs were assigned to receive or not receive losartan.

RESULTS—The level of apoptosis in the retina was higher in diabetic WKY rats than in the control group, and higher levels were found in diabetic SHRs. The apoptotic cells expressed neural and glial markers. The retinal glial reaction was more evident in diabetic WKY rats and was markedly accentuated in diabetic SHRs. Superoxide production in retinal tissue increased in diabetic WKY rats, and a greater increase occurred in diabetic SHRs. Glutathione levels decreased only in diabetic SHRs. As a consequence, the levels of nitrotyrosine and 8-hydroxy 2′-deoxyguanosine, markers of oxidative stress, were elevated in diabetic groups, mainly in diabetic SHRs. Mitochondrial integrity was dramatically affected in the diabetic groups. The ARB treatment reestablished all of the above-mentioned parameters.

CONCLUSIONS—These findings suggest that concomitance of hypertension and diabetes exacerbates oxidative stress, neurodegeneration, and mitochondrial dysfunction in the retinal cells. These data provide the first evidence of AT_1 blockage as a neuroprotective treatment of diabetic retinopathy by reestablishing oxidative redox and the mitochondrial function. *Diabetes* **58:1382–1390, 2009**

Diabetic retinopathy is a vision-threatening disease presenting neurodegenerative features associated with extensive vascular changes. At present, there is no established neuroprotective treatment that avoids visual disturbance in patients with diabetes. Earlier studies have focused on improving glycemic control for prevention and treatment of diabetic retinopathy (1,2). However, with the publication of EURODIAB EUCLID (Controlled Trial of Lisinopril in Insulin-Dependent Diabetes) (3) and U.K. Prospective Diabetes Study results (1), controlling blood pressure and, specifically, interference in the renin-angiotensin system have emerged as important strategies for treating diabetic retinopathy. More recently, DIRECT (Diabetic Retinopathy Candesartan Trial), a randomized double-blind placebo-controlled study with type 1 or type 2 diabetic patients into daily placebo or 32 mg candesartan groups, an angiotensin II receptor blocker (4,5), showed the importance of the renin-angiotensin system in diabetic retinopathy. In patients with type 1 diabetes, candesartan had a mild effect on reducing the incidence of retinopathy by 18%, and in post hoc analyses, candesartan reduced the incidence of retinopathy by three or more steps by 35%. In patients with type 2 diabetes, treatment with candesartan decreased the progression of retinopathy by 34% in participants with early retinopathy. These data showed that the potential benefits of the angiotensin II type 1 (AT_1) receptor blocker (ARB) candesartan might be seen in early stages of diabetic retinopathy.

Previous studies had demonstrated the presence of all renin-angiotensin system components in the retina (6,7). Clinical studies by Funatsu et al. (8) have showed increased angiotensin II levels in vitreous specimens of diabetic patients with retinopathy, demonstrating that the renin-angiotensin system is activated in diabetic retinopathy. Besides the vascular effects of renin-angiotensin system components, a mechanism of neuronal dysfunction involving this system was described in the diabetic retina in vivo and in vitro through phosphorylated extracellular signal–regulated kinase, downregulating synaptophysin, the major synaptic vesicle protein (9).

Diabetes increases oxidative stress, which plays a key regulatory role in the development of its complications (10,11). Reactive oxygen species (ROS) generated by high glucose are considered a causal link between elevated glucose and the pathways of development of diabetic complications (12). In the retina, mitochondrial dysfunc-

TABLE 1
Physiological parameters evaluated monthly in each of the studied groups

	n	Weeks	Body weight (g)	SBP (mmHg)	Glycemia (mmol/l)
Control WKY rats	27	0	372 ± 29	125 ± 4	8.9 ± 1.2
Diabetic WKY rats	30	0	368 ± 37	126 ± 6	35 ± 5.8*
Control SHRs	26	0	252 ± 22†	188 ± 15‡	8.6 ± 1.0
Diabetic SHRs	31	0	248 ± 15†	189 ± 13‡	36.2 ± 5.7*
Diabetic SHRs with losartan	25	0	253 ± 14†	189 ± 11‡	36.4 ± 5.8*
Control WKY rats	27	4	419 ± 26	126 ± 8	10.1 ± 1.5
Diabetic WKY rats	30	4	351 ± 19§	123 ± 2	37 ± 5.4*
Control SHRs	26	4	299 ± 44	190 ± 11‡	9.7 ± 1.8
Diabetic SHRs	31	4	235 ± 47§	191 ± 9‡	36.8 ± 5.9*
Diabetic SHRs with losartan	25	4	247 ± 36§	136 ± 6	37.2 ± 5.2*
Control WKY rats	27	8	489 ± 33	126 ± 1	9.9 ± 1.8
Diabetic WKY rats	30	8	357 ± 25§	121 ± 4	37 ± 7.1*
Control SHRs	26	8	325 ± 33	192 ± 13‡	10.1 ± 1.4
Diabetic SHRs	31	8	229 ± 30§	194 ± 15‡	37.9 ± 6.0*
Diabetic SHRs with losartan	25	8	238 ± 27§	135 ± 8	37.9 ± 6.1*
Control WKY rats	27	12	519 ± 40	124 ± 6	10.8 ± 1.7
Diabetic WKY rats	30	12	372 ± 52§	121 ± 6	38.0 ± 6.2*
Control SHRs	26	12	334 ± 25	194 ± 17‡	10.3 ± 1.5
Diabetic SHRs	31	12	210 ± 27§	197 ± 20‡	38.7 ± 6.1*
Diabetic SHRs with losartan	25	12	223 ± 28§	135 ± 7	37.8 ± 6.3*

*$P < 0.0001$ vs. respective control groups; †$P < 0.0001$ vs. WKY group; ‡$P < 0.0001$ vs. WKY groups and diabetic SHRs treated with the ARB losartan; §$P < 0.0001$ vs. respective control groups.

tion is present in hyperglycemic conditions and is an important source of superoxide production (12,13). Recently, our group has demonstrated that there is an increase in superoxide retinal production in diabetic spontaneously hypertensive rats (SHRs) concomitant with a decrease in reduced GSH, an important antioxidant system present in the retina (14). As a consequence, extensive retinal oxidative damage, evaluated by retinal tyrosine nitration and 8-hydroxy-2′-deoxiguanosine (8-OHdG), was observed (14).

Oxidative stress may lead to cell death (15) via apoptotic means, and it is widely known that apoptosis of retinal cells is a consummated phenomenon in diabetic retinopathy. Retinal capillary cells undergo accelerated apoptosis, which precedes the detection of any histopathological changes characteristic of diabetic retinopathy (16). The retinal vascular changes present in the retina from diabetic models were well documented (17,18), but some investigators have demonstrated profound retinal abnormalities, evaluated by electroretinography, and potential visual changes evoked before the onset of the first vascular change is detectable in the diabetic retina (19,20). In this regard, it has been recently reported that both apoptosis and glial activation, two characteristic features of retinal neurodegeneration, are present in the retinas of diabetic donors free of microvascular abnormalities according to the ophthalmoscopic examinations performed in the preceding 2 years (21,22). In view of the good evidence suggesting that the protective benefits of renin-angiotensin system inhibition extend beyond blood pressure control, the aim of the current study was to determine whether hypertension exacerbates oxidative stress–induced neuronal damage in the diabetic retina and whether treatment with the ARB losartan abrogates retinal neurodegeneration in diabetic hypertensive rats.

RESEARCH DESIGN AND METHODS

The protocol complies with the guidelines of the Brazilian College of Animal Experimentation (COBEA) and the Statement for the Use of Animals in Ophthalmic and Vision Research (ARVO), and it was approved by the local committee for ethics in animal research (CEEA/IB/Unicamp). The SHRs and normotensive control Wistar Kyoto (WKY) rats used were provided by Taconic (Germantown, NY) and bred in our animal facility. The rats were housed at a constant temperature (22°C) on a 12-h light/dark cycle with ad libitum access to food and tap water.

Experimental diabetes was induced in 12-week-old hypertensive male SHRs and WKY rats with a single intravenous injection of streptozotocin (50 mg/kg in sodium citrate buffer, pH 4.5; Sigma, St. Louis, MO). From the day after diabetes induction, the diabetic SHRs were randomly assigned to receive no antihypertensive treatment or to be treated with the ARB losartan (200 mg/l; Merck Sharp & Dome Farmaceutica, São Paulo, Brazil) in drinking water. During the study, diabetic rats received 2 units of insulin (human insulin HI-0310; Lilly) three times per week subcutaneously to promote survival and prevent ketoacidosis. Control rats received only vehicle. Blood glucose levels were measured by the colorimetric GOD-PAP assay (Merck, Darmstadt, Germany). Values ≥15 mmol/l were indicative of diabetes. Systolic blood pressure (SBP) was obtained by tail-cuff plethysmography (Physiograph MK-III-S; Narco Bio-System, Houston, TX) as previously reported (14). Body weight, blood glucose levels, and SBP were measured at 0, 4, 8, and 12 weeks of duration of diabetes. At 12 weeks after diabetes induction, the rats were killed, and the retinas in one eye were detached from the retinal pigmented epithelium cell layer and used for protein extraction or colorimetric assays; the other eye was used for immunohistochemical or immunofluorescence assays.

Terminal deoxynucleotidyl transferase–mediated dUTP nick-end labeling. To determine whether retinal cell apoptosis was influenced by diabetes or rat strain, the terminal deoxynucleotidyl transferase (TdT)–mediated dUTP nick-end labeling (TUNEL) method for detecting DNA breaks in situ was applied to retinal tissue. After quenching endogenous peroxidase, the sections were rinsed in One-Phor-All buffer (Amersham Pharmacia Biotech, Piscataway, NJ) and incubated with TdT (Amersham Pharmacia Biotech) and biotinylated dUTP (Gibco/BRL, Life Technologies, Grand Island, NY) in TdT buffer. Labeled nuclei were detected with ABC Vectastain (Vector Laboratories, Burlingame, CA) and diaminobenzidine tetrahydrochloride/chloride/hydrogen peroxide and counterstained with hematoxylin. As a positive control, some slides were treated with DNase (Sigma). The quantitative analysis for TUNEL-positive cells was performed by an observer with no knowledge of the studied groups and expressed as the number of positive cells per retinal section.

Double-immunofluorescence for caspase-3 and glial fibrillary acidic protein or nestin to identify the cell type origin. The eyes were enucleated and fixed with 4% paraformaldehyde, cryoprotected in 30% sucrose in phosphate buffer, frozen in embedding medium (OCT; Sakura Finetek, Torrance, CA), and cut perpendicularly to the vitreal surface. The slides were blocked with BSA and the sections were stained with both primary antibodies to polyclonal cleaved caspase-3 (1:10; Cell Signaling), a marker of apoptosis, and polyclonal anti–glial fibrillary acidic protein (GFAP) antibody (1:10; Santa Cruz Biotechnology, Santa Cruz, CA) for Müller glial cell or anti-rat nestin monoclonal antibody (1:10; BD Pharmingen, Franklin Lakes, NJ) for neural cell identification. The sections were then incubated with the appropriate secondary antibodies. Afterwards, the sections were rinsed and cover-slipped with Vectashield antifading medium containing 4′,6′-diamino-2-phenylindole used for nuclei staining (Vector). The sections were examined with a confocal laser scanning microscope (LSM510; Zeiss) using appropriate emission filters. Digital images were captured using specific software (LSM; Zeiss).

Immunofluorescence for GFAP for estimation of glial reaction on retinal tissue. The immunofluorescence labeling of GFAP was performed as described above in double-immunofluorescence staining assay. The sections were examined using an Olympus BX51 fluorescence microscope. Digital images were captured using specific software (Image Pro Express 6.0). The GFAP analyses were determined using the public domain program Image J (National Institutes of Health, available online at http://rsb.info.nih.gov/ij). The semiquantitative analyses were performed as mentioned above in TUNEL assay. The fluorescence of GFAP was expressed as the percentage of fluorescence per millimeter squared of retina.

Detection of superoxide anion production in retinal tissue. Lucigenin (bis-N-methylacridinium nitrate; Invitrogen, Eugene, OR) was used to measure superoxide anion production (23). Briefly, the retinas were isolated and placed into tubes containing RPMI-1640 medium (Gibco/BRL, Life Technologies, Gaithersburg, MD) at 37°C in a humidified atmosphere of 95% air/5% CO_2. Then, 25 mmol/l of lucigenin was added, and photon emission was measured over 10 s; repeated measurements were made over a 3-min period using a luminometer (TD 20-E; Turner). Superoxide production was expressed as the relative luminescence units (RLU) per minute per milligram protein. Protein concentration was measured using the Bradford method (24) using BSA standard.

Determination of reduced glutathione levels in the retina. Retinal glutathione (GSH) levels were measured using a method described previously (25), with a few modifications described previously (14). The absorbance was read at 412 nm and the GSH concentration expressed as micromoles per liter GSH per microgram of retinal protein. GSH was used as an external standard for preparation of a standard curve.

Immunohistochemistry for nitrotyrosine and 8-OHdG in retinal slides. Briefly (14), after quenching endogenous peroxidase, the sections were incubated with nonfat milk. Tissue sections were incubated with polyclonal rabbit anti-nitrotyrosine antibody (Upstate Cell Signaling Solutions, Lake Placid, NY) and a mouse monoclonal anti–8-OHdG antibody (1:50, N45.1; Japan Institute for the Control of Aging). Afterwards, secondary appropriated antibodies were applied to the sections. Labeled nuclei were detected as described above in the section on immunohistochemistry for TUNEL. Staining was performed, omitting the primary antibody for negative controls. For nitrotyrosine, quantitative analyses were performed as a positivity percentage in all retinal layers, grading from 0 for no positivity to 4 for ≥80% of positivity (14). The 8-OHdG analyses were determined using the public domain program Image J (National Institutes of Health) and expressed by percentage of positivity per retinal field. Semiquantitative analyses were performed as described above in the section on GFAP immunofluorescence assay.

Western blotting analysis for Bcl-2 protein. The retinas were lysed in a buffer containing 2% SDS and 60 mmol Tris-HCl (pH 6.8) supplemented with a protease inhibitor cocktail (Complete; Boehringer-Mannheim, Indianapolis, IN). After centrifugation, the protein concentrations were measured by the Bradford method. For analysis, 100 μg of total retinal protein was loaded into SDS polyacrylamide gels. Molecular weight markers (Rainbow; Amersham Pharmacia) were used as standards. Proteins were transferred to nitrocellulose membranes (Bio-Rad, Hercules, CA). Membranes were blocked in nonfat milk, incubated with primary antibody (rabbit polyclonal anti–Bcl-2; Santa Cruz), subsequently incubated with goat anti-rabbit IgG horseradish peroxidase (HRP) secondary antibody, and developed by chemiluminescence method (Super Signal CL-HRP substrate system; Pierce, Rockford, IL). Exposed films were scanned with a densitometer (Bio-Rad) and analyzed quantitatively with Multi-Analyst Macintosh Software for Image Analysis Systems. Equal loading and transfer were ascertained by reprobing the membranes for β-actin.
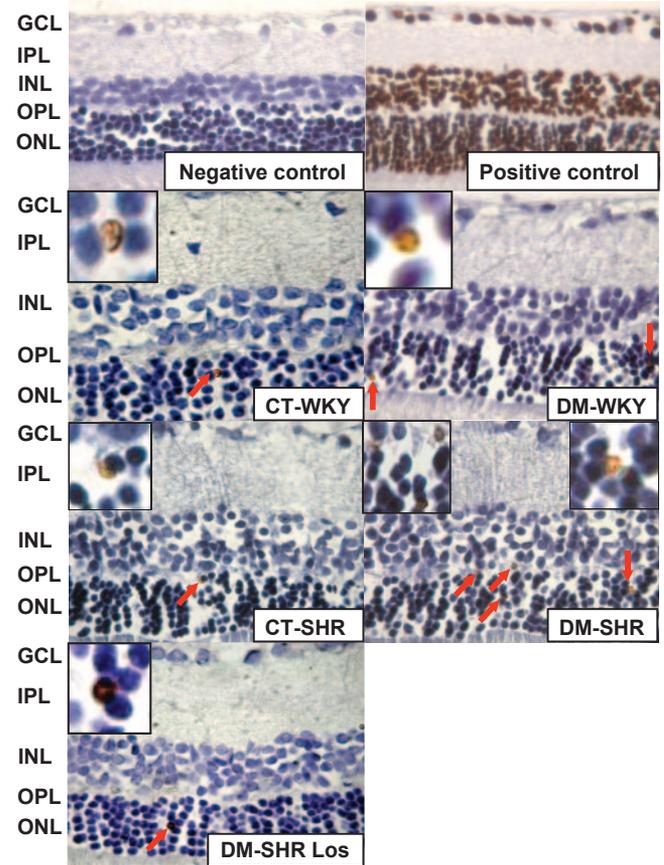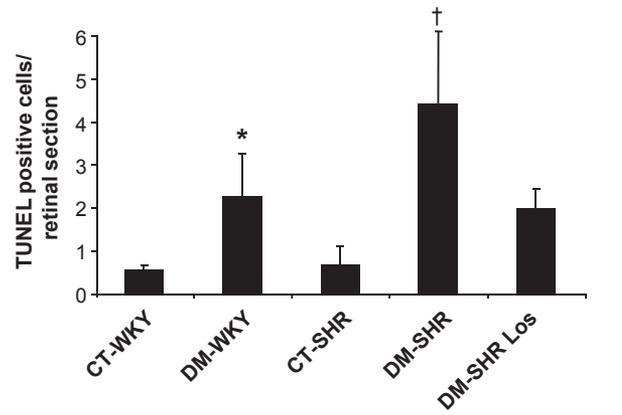
FIG. 1. *A*: A representative immunohistochemical identification of TUNEL-positive cells in the retinal sections of control and diabetic WKY rats and SHRs and losartan-treated diabetic SHRs. The positive controls were retinal slides treated with DNase. The majority of positive cells were localized in the outer nuclear layer of the retina, indicating, therefore, that the photoreceptors are the most affected cells. *B*: Summary of the number of TUNEL-positive cells per retinal section (0.5 ± 0.1 vs. 2.3 ± 0.9 positive cells per retinal section for control WKY vs. diabetic WKY rats, *P* = 0.03; 2.3 ± 0.9 vs. 4.4 ± 2.0 positive cells per retinal section for diabetic WKY rats vs. diabetic spontaneously hypertensive rats, *P* = 0.01; 0.6 ± 0.3 vs. 4.4 ± 2.0 positive cells per retinal section, control spontaneously hypertensive vs. diabetic spontaneously hypertensive, *P* = 0.0003; 4.4 ± 2.0 vs. 2.0 ± 0.4 positive cells per retinal section for diabetic spontaneously hypertensive vs. diabetic spontaneously hypertensive–losartan, *P* = 0.01). **P* = 0.03; †*P* = 0.01. CT, control; DM, diabetic; GCL, ganglion cell layer; INL, inner nuclear layer; IPL, inner plexiform layer; Los, losartan; ONL, outer nuclear layer; OPL, outer plexiform layer. (A high-quality digital representation of this figure is available in the online issue.)

Immunoprecipitation of retinal protein extract for mitochondrial uncoupling protein-2. The retinas were lysed directly with buffer A containing 100 mmol/l Tris, 10 mmol/l sodium pyrophosphate, 100 mmol/l sodium
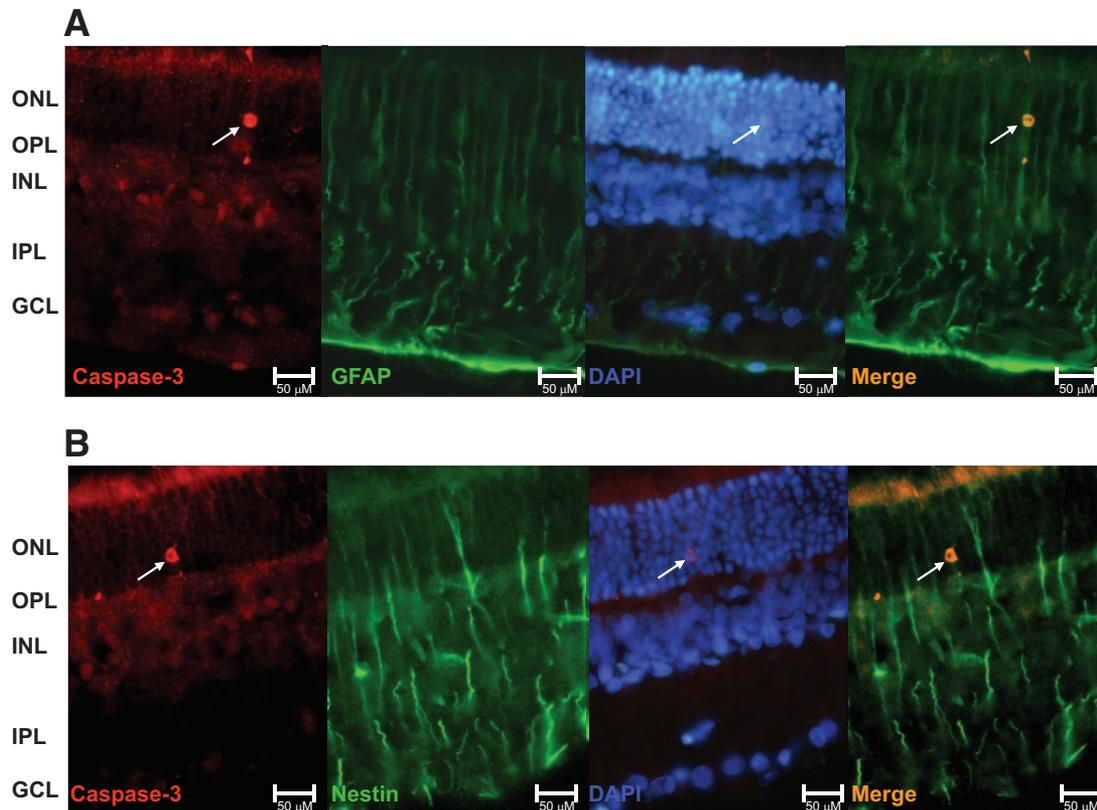
FIG. 2. *A*: Retinal section with a caspase-3–positive cell colabeled with GFAP antigen localized on outer nuclear layer, as indicated by the arrow. This is indicative of the glial nature of the apoptotic cell. *B*: Caspase-3–positive cell expressing the intermediate filament nestin in the outer nuclear layer of the retina, demonstrating the neural origin of the indicated cell. Scale bars = 50 μm. Both double-labeling immunofluorescence assays were performed in retinal tissue obtained from diabetic hypertensive rats because of its higher number of TUNEL-positive cells observed. DAPI, 4′,6′-diamino-2-phenylindole; GCL, ganglion cell layer; INL, inner nuclear layer; IPL, inner plexiform layer; ONL, outer nuclear layer; OPL, outer plexiform layer. (A high-quality digital representation of this figure is available in the online issue.)

fluoride, 10 mmol/l EDTA, 2 mmol/l phenylmethylsulfonyl fluoride, 10 mmol/l sodium ortovanadate, and 1% Triton X-100. The protein concentrations were measured by the Bradford method (24). Samples containing 1 mg of total protein were incubated with antibody goat polyclonal IgG uncoupling protein-2 (UCP-2; Santa Cruz) overnight, followed by the addition of protein A Sepharose for 1 h. After centrifugation, the pellets were repeatedly washed in buffer C (100 mmol/l Tris, 10 mmol/l sodium vanadate, 10 mmol/l EDTA, and 1% Triton X-100). For immunoblotting, 400 μg of protein was loaded into 5% glycerol/0.03% bromophenol blue/10 mmol dithiothreitol and then loaded onto 15% SDS polyacrylamide gels. Molecular weight markers were used as standards. Proteins were transferred to nitrocellulose membranes (Bio-Rad), and the membranes were blocked in nonfat milk and then incubated with primary antibody goat polyclonal IgG UCP-2 (1:500). The blots were subsequently incubated with secondary antibody donkey anti-goat IgG HRP and developed using a chemiluminescence method. Equal loading and transfer were ascertained by Ponceau S staining.

Statistical analysis. The results are expressed as the means ± SD. The groups were compared by one-way ANOVA, followed by the Fisher protected least-significant difference test. StatView statistics software for Macintosh was used for all comparisons with a significance value of $P < 0.05$.

RESULTS

Physiological characteristics of the studied groups. The final body weight was lower after streptozotocin injection in both WKY and SHRs ($P < 0.0001$), and it was not affected by treatment with losartan in diabetic SHRs. As expected, SBP was significantly higher in SHRs than in WKY rats, and it was reduced in the treated SHRs ($P < 0.0001$). Blood glucose levels were higher in diabetic rats compared with nondiabetic groups, and these were not modified by ARB treatment ($P < 0.0001$) (Table 1).

TUNEL staining is modified by diabetes or rat strain. TUNEL staining was a rare event in the retina from control rats. After 12 weeks of diabetes in WKY rats, an increment of retinal cells staining positive for TUNEL was observed ($P = 0.03$). The diabetic SHRs exhibited an increased number of TUNEL-positive cells in the retina compared with diabetic WKY rats ($P = 0.01$) and control SHRs ($P = 0.0003$). Losartan significantly reduced the number of TUNEL-positive cells in all retinal layers compared with diabetic SHRs ($P = 0.01$) (Fig. 1).

Identification of apoptotic cell type. To further characterize the apoptotic cells in the retina of adult rats, we labeled retinal sections for GFAP and nestin. A caspase-3–positive cell colabeled with the GFAP marker was observed (Fig. 2*A*), and another caspase-3–positive cell expressed nestin (Fig. 2*B*); both cells were in the outer nuclear layer. These findings indicate that the apoptotic retinal cells are of glial and neural origin.

Immunofluorescence for detection of glial reactivity induced by diabetes and hypertension. Retinal glial reaction, demonstrated by a local increase in GFAP expression, is an early marker in the pathogenesis of diabetic retinopathy (26). In the retina of control WKY rats, GFAP positivity is minimally apparent. In contrast, after diabetes induction there was an accentuated increase in glial reactivity ($P < 0.0001$). Similarly observed in diabetic WKY rats, there was a moderate glial reaction throughout the retina in control SHRs ($P = 0.4$), and the concomitance of both diabetes and hypertension extensively exacerbated
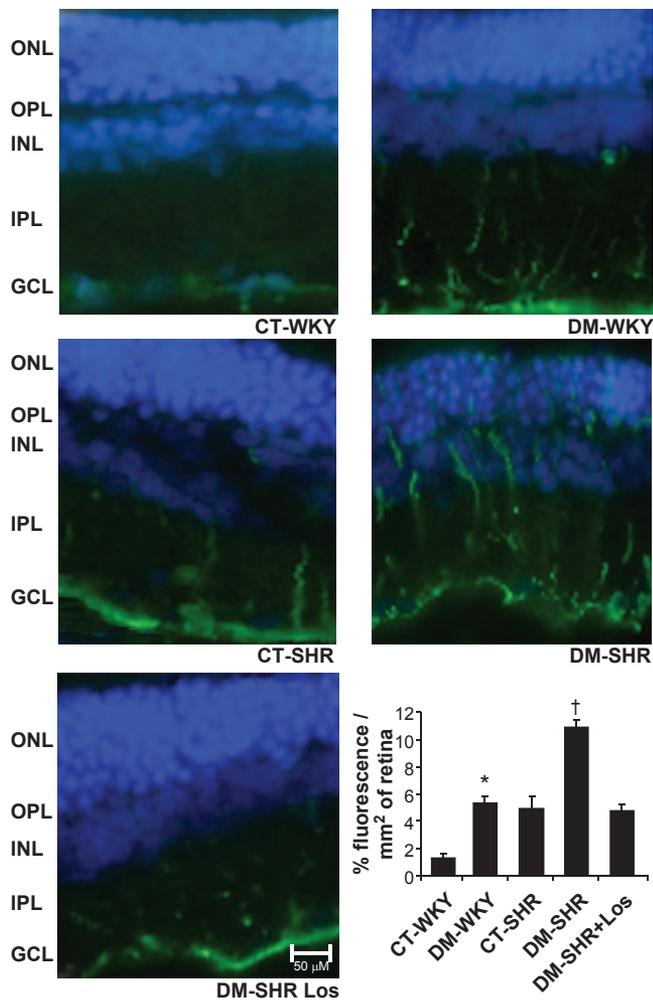
FIG. 3. Evaluation of glial cell reactivity by GFAP immunofluorescence in retinas of control and diabetic WKY and spontaneously hypertensive rats. The presence of diabetes or hypertension alone induced a clear increase in GFAP immunoreactivity throughout the retina. The concomitance of both provoked a further increase in glial reactivity, and the losartan treatment abolished this effect. Bars = means ± SD of percentage of fluorescence per millimeter squared of retina. Scale bars = 50 μm. The graph shows 1.3 ± 0.3 vs. 5.3 ± 0.5% of fluorescence/mm^2 of retina for control WKY vs. diabetic WKY rats, *$P <$ 0.0001; 5.3 ± 0.5 vs. 4.9 ± 0.08% of fluorescence/mm^2 of retina for diabetic WKY rats vs. control SHRs, $P = 0.4$; 4.9 ± 0.08 vs. 10.8 ± 0.5% of fluorescence/mm^2 of retina for control SHRs vs. diabetic SHRs, †$P <$ 0.0001; 10.8 ± 0.5 vs. 4.7 ± 0.5% of fluorescence/mm^2 of retina for diabetic SHRs vs. diabetic losartan (Los)-treated SHRs, †$P <$ 0.0001. CT, control; DM, diabetic; GCL, ganglion cell layer; INL, inner nuclear layer; IPL, inner plexiform layer; ONL, outer nuclear layer; OPL, outer plexiform layer. (A high-quality digital representation of this figure is available in the online issue.)

the GFAP staining in retinal tissue ($P <$ 0.0001). The treatment prevented the retinal glial reaction seen in diabetic SHRs, which remained similar to control levels ($P <$ 0.0001) (Fig. 3).

Superoxide anion production and GSH levels. After 12 weeks of diabetes, a significant increase of superoxide anion production was observed in diabetic WKY rats compared with the control WKY rats (0.9 ± 0.3 vs. 2.0 ± 0.8 RLU · min^{-1} · mg protein^{-1}, $P = 0.03$), and the concomitance of diabetes and hypertension exacerbated the superoxide production compared with the other groups ($P = 0.0002$). To identify the source of superoxide production, we used diphenyliodonium, an inhibitor of flavin-containing oxidases, and rotenone, an inhibitor of
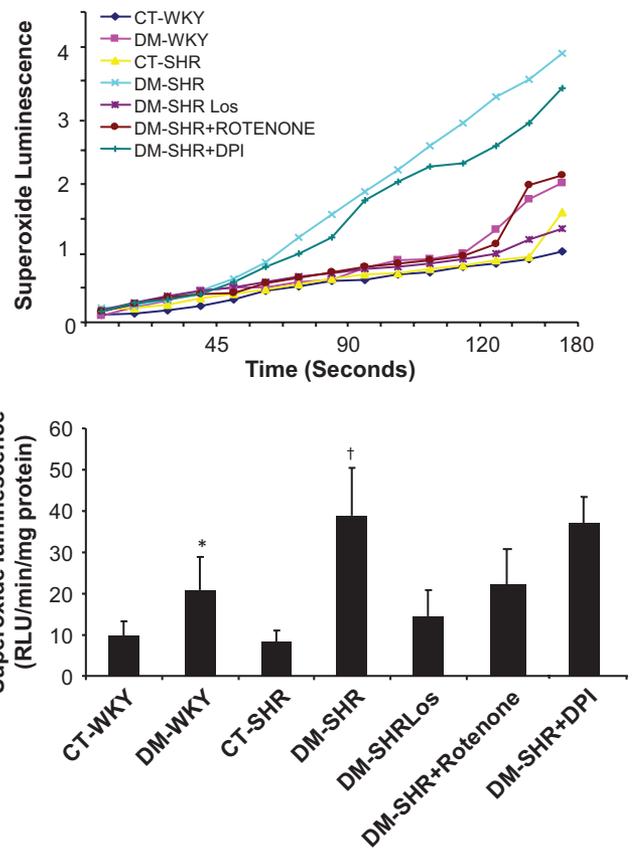
FIG. 4. Total superoxide generation in retinal tissue. Superoxide anion generation of retinal tissue was determined by the lucigenin-enhanced chemiluminescence method, and photoemission was measured every 10 s for 3 min. The peak level of superoxide generation was observed ~3 min after lucigenin was added to the reaction buffer containing retina from different groups. Diabetes increased superoxide production (RLU · min^{-1} · mg protein^{-1}) in the retina, and the concomitance of diabetes and hypertension further exacerbated this parameter. The presence of diphenyliodonium (20 μmol/l), an inhibitor of flavin-containing oxidases, did not affect superoxide production, whereas preincubation with rotenone (100 μmol/l) resulted in a marked reduction in superoxide production from retinal tissue. This indicates that mitochondria are an important source of the superoxide in retina tissue. Treatment with the ABR losartan reduced superoxide production to levels observed in the control groups. Bars are the means ± SD. *$P = 0.03$ vs. control WKY; †$P = 0.0002$ vs. other groups. CT, control; DM, diabetic; DPI, diphenyliodonium.

complex I of the mitochondrial respiratory chain, in vials containing retina from diabetic SHRs. Preincubation of the retinal tissue with diphenyliodonium (20 μmol/l) did not affect superoxide production, whereas preincubation with rotenone (100 μmol/l) resulted in a marked reduction in superoxide production. This indicates that mitochondria are an important source of the superoxide in retinal tissue (Fig. 4A). Therefore, we evaluated the effect of the treatment with losartan on retinal superoxide production. It was observed that the ARB restored the superoxide production in retina in diabetic SHRs to control WKY levels ($P = 0.0003$) (Fig. 4B).

Antioxidant defense was examined using the quantitative measurement of GSH levels in the retinal tissue; it was diminished in diabetic WKY rats compared with control WKY rats, but not significantly ($P = 0.1$). However, the concomitance of diabetes and hypertension led to a marked diminution in GSH concentration (~2.5-fold decrease) compared with control SHRs ($P = 0.0005$). The treatment with losartan reestablished this parameter to control SHR levels ($P = 0.006$) (Fig. 5).
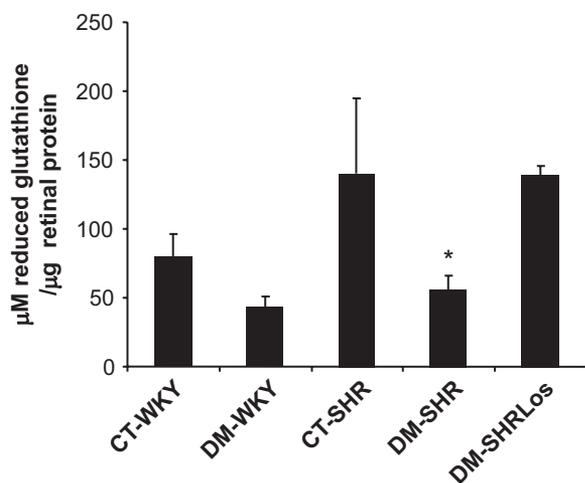
FIG. 5. Concentration of reduced GSH from retinas of control and diabetic WKY and SHR rats and treated diabetic SHRs (μmol/l GSH per μg of retinal protein). There was a significant decrease in GSH levels in diabetic SHRs compared with control SHRs; the ARB treatment in diabetic hypertensive rats prevented this reduction. Bars = means ± SD (79 ± 17 vs. 43 ± 7 μmol/l reduced GSH per μg retina protein for control WKY vs. diabetic WKY rats, $P = 0.1$; 140 ± 54 vs. 56 ± 10 μmol/l reduced GSH per μg retina protein for control SHRs vs. diabetic SHRs, $P = 0.0005$). *$P = 0.006$. CT, control; DM, diabetic; Los, losartan.

Diabetes elevated the nitrosative imbalance and was prevented by ARB treatment in diabetic SHRs. The nitration of tyrosine, an effect of peroxynitrite on proteins, was assessed by nitrotyrosine expression. The immunohistochemistry for nitrotyrosine showed stronger staining throughout retinal layers in diabetic WKY rats and control SHRs compared with control WKY rats ($P < 0.0001$ and $P = 0.0003$, respectively). The presence of diabetes alone showed an increment in nitrotyrosine values compared with hypertension alone ($P = 0.004$). The concomitance of diabetes and hypertension further increased nitrotyrosine expression in all retinal layers compared with other groups ($P = 0.001$). Losartan completely reestablished retinal nitrosative status in the retinas of diabetic SHRs ($P < 0.0001$). These findings suggest that losartan protects the retinal tissue against nitrosative stress in diabetic SHRs (Fig. 6A).

Oxidative DNA damage in diabetic SHR retina was prevented by treatment with losartan. The distribution of positive 8-OHdG, a marker of oxidative damage on nucleic acids, was heterogeneous in retinal tissue, presenting higher positivity in the outer nuclear layer of diabetic WKY rats and in all cellular layers of diabetic SHRs. The presence of diabetes or hypertension alone induced a significant increment in 8-OhdG–positive cells in retinal tissue compared with the control WKY group ($P = 0.003$). The concomitance of both resulted in a marked increase in oxidative DNA damage compared with control SHRs ($P < 0.0001$). Similarly, as observed with nitrotyrosine, losartan significantly protected the retinal cells against DNA damage ($P < 0.0001$) (Fig. 6B).

Diabetes induced retinal mitochondrial dysfunction and was prevented by losartan. The overexpression of Bcl-2 mitochondrial protein inhibits the release of cytochrome c into the cytosol, protecting the cells against early death (27). Therefore, the estimation of Bcl-2 may be indicative of mitochondrial involvement in the apoptotic cascade. The expression of Bcl-2 in total retinal lysates was decreased in both diabetic groups when compared

with the controls ($P = 0.01$) and reestablished in diabetic SHRs treated with losartan (Fig. 7A).

UCP-2 expression reflects the mitochondrial energy metabolism and might play a role in retinal neurodegeneration (28). Similarly, as observed in Bcl-2 protein, the expression of UCP-2 was diminished in both diabetic groups compared with the respective control groups ($P = 0.03$), and it was restored to the levels of the control groups in losartan-treated diabetic SHRs ($P = 0.04$) (Fig. 7B).

DISCUSSION

The ARB used in the treatment of hypertension exerts a variety of pleiotropic effects, including antioxidant, anti-apoptotic, and anti-inflammatory effects (29). However, the possible antioxidant/antiapoptotic effects of ARB in the diabetic retina have never been addressed. In the current study, we investigated the potential effect of the losartan on retinal neurodegeneration in a model that combines diabetes and hypertension. We observed that the apoptotic rate was higher in the retina of diabetic SHRs compared with control WKY rats, and the cells exhibited neural and glial characteristics, as demonstrated by specific antigens. The oxidative imbalance, characterized by an increase in superoxide production and a decrease in reduced GSH levels in retinal tissue, was higher in diabetic rats and accentuated in diabetic SHRs in the presence of mitochondrial involvement, as demonstrated by decreased expression of Bcl-2 and UCP-2 mitochondrial proteins. Losartan treatment led to amelioration of the apoptotic rate in neural and glial retinal cells, reestablishment of redox status by decreasing superoxide production and improving the antioxidative enzymatic system GSH, and restoration of mitochondrial protein expression levels. Therefore, the ARB seemed to offer neural protection, including antiapoptotic and antioxidant benefits, in the retina of diabetic hypertensive rats.

The increased number of TUNEL-positive cells detected in the retinas of diabetic SHRs occurred mainly in the outer nuclear layer, and this may contribute to widespread retinal dysfunction. In line with previous studies of electroretinography, Phipps et al. (30) demonstrated a significant reduction in the rod photoreceptor response in diabetic Ren-2 rats compared with nondiabetic Ren-2 rats, which in turn translated losses to b-wave and oscillatory potentials. Other studies had confirmed that rod photoreceptors are the primary retinal neuron affected by diabetes (31,32). The photoreceptors are most vulnerable to oxidative damage because of the high content of polyunsaturated fatty acids in their membranes; oxidative stress may cause lipid peroxidation reactions (33) and therefore damage their structure and function. In this study, we observed glial reactivity, as evaluated by GFAP immuno-reactions, but not apoptosis of photoreceptor, as evaluated by TUNEL, in hypertensive rats. This is explained by the fact that glial cells and photoreceptors are damaged by oxidative stress through different mechanisms. The glial cells possess mechanisms providing high intracellular GSH concentration (34). Depending on the insult, the depletion of GSH in glial cells and the subsequent heme oxygenase-1 induction (35) is associated with the production of bilirubin, a potent free radical scavenger (36), and with the reduction of heme, a powerful pro-oxidant (37). One reason for this is that Müller cells provide metabolic
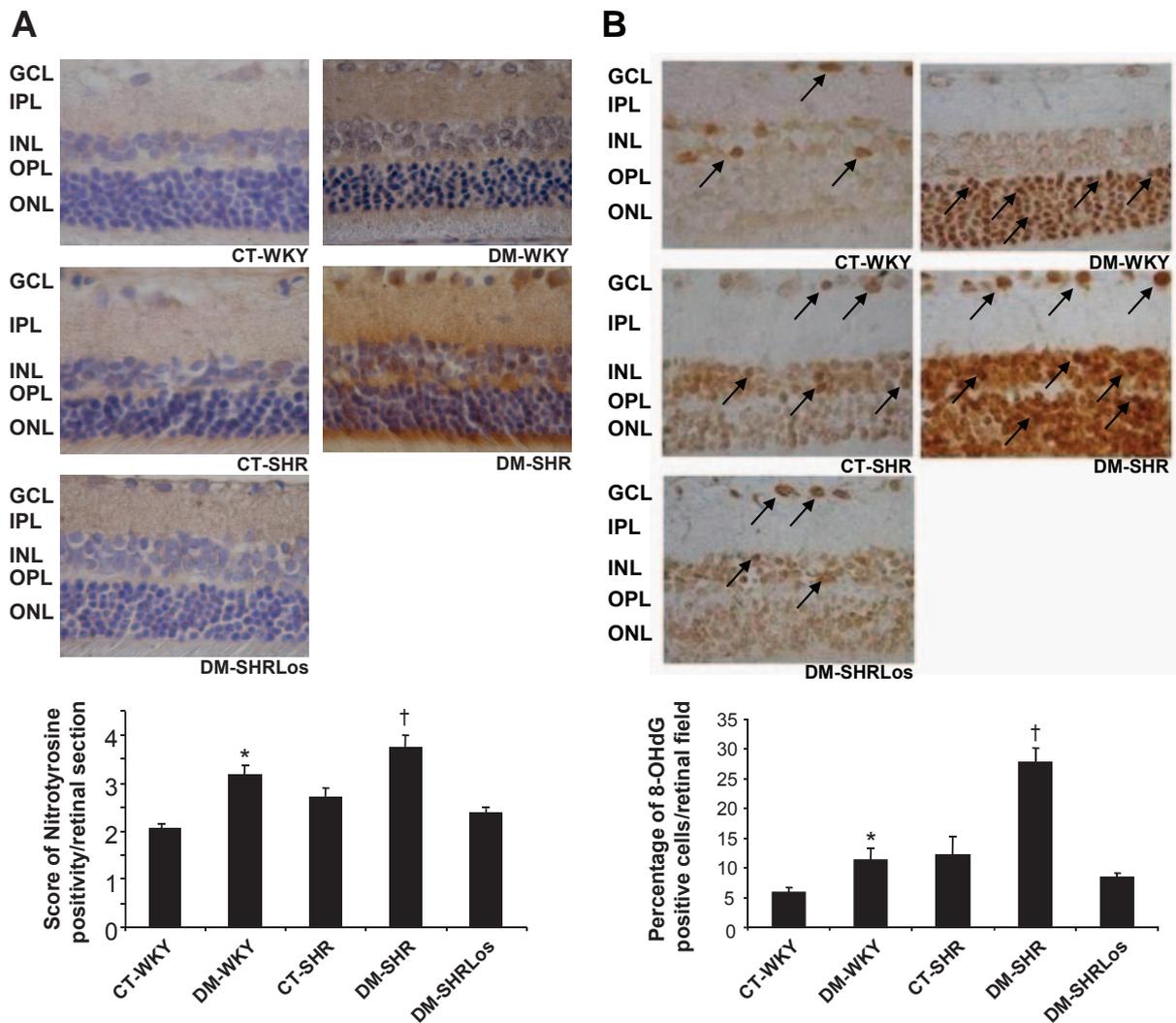
FIG. 6. *A*: Representative photomicrograph of immunolocalization of nitrotyrosine in control and diabetic WKY and SHRs and diabetic SHRs treated with losartan. The presence of nitrotyrosine is indicated by the brown color, and the positivity is diffuse. Bars represent the means ± SD of score of positivity of nitrotyrosine per retinal section, as defined in RESEARCH DESIGN AND METHODS. Diabetes increased tyrosine nitration in retinal tissue, and concomitance of diabetes and hypertension exacerbates this phenomenon. A significant reduction was observed in treated diabetic SHRs. The graph shows 2.0 ± 0.1 vs. 3.2 ± 0.2 score of positivity for control WKY vs. diabetic WKY rats, *$P < 0.0001$; 2.0 ± 0.1 vs. 2.7 ± 0.2 score of positivity for control WKY vs. control SHRs, $P = 0.0003$; 3.2 ± 0.2 vs. 2.7 ± 0.2 score of positivity for diabetic WKY rats vs. control SHRs, $P = 0.004$). †$P = 0.001$ vs. other groups. *B*: Representative photomicrograph of immunohistochemistry for 8-OHdG from retinas of control and diabetic WKY and SHRs and diabetic SHRs treated with losartan. Bars represent the means ± SD of percentage of positive 8-OHdG retinal cells per retinal field, as defined in RESEARCH DESIGN AND METHODS. The presence of 8-OHdG is indicated by the brown color, and the positivity is in the nucleus of the cells. The presence of diabetes or hypertension separately increased the oxidative DNA damage in retinal cell layers, and concomitance of both induced a markedly pronounced effect; the antihypertensive treatment with ARB promoted significant neuroprotection of retinal tissue, abolishing this damage. All the retinal layers were included in the quantitation for both proteins. *$P = 0.003$ vs. control WKY; †$P < 0.0001$ vs. other groups. CT, control; DM, diabetic; GCL, ganglion cell layer; INL, inner nuclear layer; IPL, inner plexiform layer; Los, losartan; ONL, outer nuclear layer; OPL, outer plexiform layer. (A high-quality digital representation of this figure is available in the online issue.)

support to adjacent neural cells, providing protective mechanisms for photoreceptors.

Previous studies demonstrated that local angiotensin II expression was extremely elevated during retinal inflammation, thereby influencing the condition of the retinal neural and vascular cells through AT_1 receptor signaling. The ARB was effective in keeping the retinal neural cells from losing their physiological activities and normal electroretinography responses; therefore, the ARB plays a key role in neuroprotection, and it preserves good visual function by reducing inflammatory reactions in the retinal neural and vascular cells, preventing the development of diabetic retinopathy (7,38). This treatment also reduced the accumulation of one of the advanced glycation end products as well as vascular endothelial growth factor

expression in a model of type 2 diabetes (39). Other studies also showed that treatment with ARBs in hypertensive diabetic Ren-2 rats prevented acellular capillary and endothelial cell proliferation as well as development of neuronal deficits in diabetes, namely loss of function in photoreceptors and neurons, independent of controlling hypertension (30,40). These findings support the concept that ARBs may be useful as a therapeutic target for diabetic retinopathy. Although in this study we did not treat the diabetic SHRs with another antihypertensive drug that does not act on the renin-angiotensin system, to avoid the hypotensive effect of the losartan treatment, the normotensive diabetic WKY rats still had markers of oxidative stress and mitochondrial dysfunctions that were not present in diabetic SHRs treated with losartan.

A

B
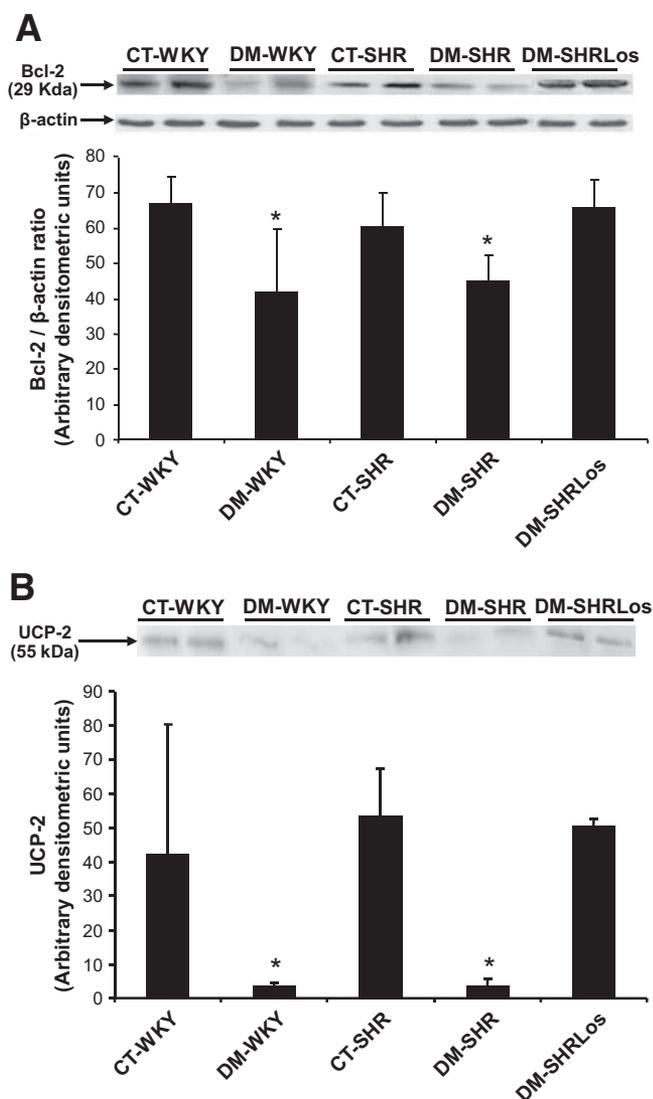
FIG. 7. *A*: **Western blot analysis of Bcl-2 in total retinal lysated of the studied groups; the bars represent the means ± SD of band densities expressed in arbitrary densitometric units from at least three independent experiments. *$P < 0.05$.** *B*: **Western blot analysis of UCP-2 in immunoprecipitated retinal protein of the studied groups. The bars represent the means ± SD of band densities expressed in arbitrary densitometric units from at least three independent experiments. *$P = 0.03$. CT, control; DM, diabetic; Los, losartan.**

The marked effect in reducing the oxidative damage in diabetic retinal tissue of hypertensive rats treated with losartan may be attributable to its antioxidant effect through ARB and an increase in nitric oxide (NO) biodisponibility via the angiotensin II type 2 receptor (41). A recent study demonstrated that intravenous application of angiotensin II reduces plasma NO levels and increases the peroxynitrite concentration, which significantly increases nitrosative stress. Treatment with valsartan, an ARB similar to losartan, suppressed this effect (42). The question of how NO can attenuate oxidative damage is still intriguing. A previous study provided direct evidence that NO inactivates xanthine oxidase by reacting first with the superoxide anion to form peroxynitrite, which in turn reduces both xanthine oxidase activity and superoxide generation (43), thus reestablishing the oxidative status.

It was previously demonstrated that hyperglycemia-induced production of ROS is associated with the devel-

opment of diabetic microvascular complications (11) and that the normalization of mitochondrial superoxide production blocks the pathways of diabetic damage (44). Normalization of mitochondrial ROS production prevents pathways involved in the development of diabetic microvascular complications (44). In the current study, the blockage of mitochondria complex I using rotenone revealed a significant reduction in its superoxide production. This fact may be explained by the observation of diversity in electron chain transport components present in different neuron subpopulations, as demonstrated by a study where mitochondria from retinal ganglion cells decreased the superoxide production in response to rotenone (45).

Mitochondria are a major endogenous source and target of superoxide and hydroxyl radicals (46). Reactive oxidant intermediates can trigger mitochondria to release cytochrome c, resulting in activation of caspase-3 (27,46). Increasing evidence indicates that mitochondria are intimately associated with the initiation of apoptosis (47,48). In this study, mitochondrial integrity was evaluated by determining Bcl-2 and UCP-2 protein expressions. The mechanism that involves angiotensin II in mitochondrial ROS production is supported by the fact that in vivo preconditioning effects of angiotensin II for cardiac ischemia/reperfusion injury may be mediated by cardiac mitochondria–derived ROS enhanced by NAD(P)H oxidase (49). The superoxide production via NAD(P)H oxidase stimulates the opening of reconstituted mitochondrial ATP-sensitive K^+ channels via a direct action on the sulfhydryl groups of this channel (50). Thus, the overstimulation of angiotensin II and renin-angiotensin system may account for mitochondrial dysfunction, in line with the observed effect that AT_1 blockage with losartan reestablished the UCP-2 and Bcl-2 contents in retinal tissue.

In summary, the findings of this study provides evidence for the first time of the benefits of the AT_1 blocker losartan in ameliorating diabetic retinal neurodegeneration, mitochondrial function, and oxidative balance.

ACKNOWLEDGMENTS

REFERENCES

1. UK Prospective Diabetes Study Group: Tight blood pressure control and risk of macrovascular and microvascular complications in type 2 diabetes: UKPDS 38. BMJ 1998;317:703–713
2. Klein R, Klein BE, Moss SE, Cruickshanks KJ. The Wisconsin Epidemiologic Study of Diabetic Retinopathy. XVII. The 14-year incidence and progression of diabetic retinopathy and associated risk factors in type 1 diabetes. Ophthalmology 1998;105:1801–1815
3. Chaturvedi N, Sjolie AK, Stephenson JM, Abrahamian H, Keipes M, Castellarin A, Rogulja-Pepeonik Z, Fuller JH. Effect of lisinopril on progression of retinopathy in normotensive people with type 1 diabetes. The EUCLID Study Group. EURODIAB Controlled Trial of Lisinopril in Insulin-Dependent Diabetes Mellitus. Lancet 1998;351:28–31
4. Chaturvedi N, Porta M, Klein R, Orchard T, Fuller J, Parving HH, Bilous R, Sjølie AK; DIRECT Programme Study Group: Effect of candesartan on prevention (DIRECT-Prevent 1) and progression (DIRECT-Protect 1) of

retinopathy in type 1 diabetes: randomised, placebo-controlled trials. Lancet 2008;372:1394–402

5. Sjølie AK, Klein R, Porta M, Orchard T, Fuller J, Parving HH, Bilous R, Chaturvedi N; DIRECT Programme Study Group: Effect of candesartan on progression and regression of retinopathy in type 2 diabetes (DIRECT-Protect 2): a randomised placebo-controlled trial. Lancet 2008;372:1385–1393

6. Danser AH, van den Dorpel MA, Deinum J, Derkx FH, Franken AA, Peperkamp E, de Jong PT, Schalekamp MA. Renin, prorenin, and immunoreactive renin in vitreous fluid from eyes with and without diabetic retinopathy. J Clin Endocrinol Metab 1989;68:160–167

7. Nagai N, Izumi-Nagai K, Oike Y, Koto T, Satofuka S, Ozawa Y, Yamashiro K, Inoue M, Tsubota K, Umezawa K, Ishida S. Suppression of diabetes-induced retinal inflammation by blocking the angiotensin II type 1 receptor or its downstream nuclear factor-kappaB pathway. Invest Ophthalmol Vis Sci 2007;48:4342–4350

8. Funatsu H, Yamashita H, Nakanishi Y, Hori S. Angiotensin II and vascular endothelial growth factor in the vitreous fluid of patients with proliferative diabetic retinopathy. Br J Ophthalmol 2002;86:311–315

9. Kurihara T, Ozawa Y, Nagai N, Shinoda K, Noda K, Imamura Y, Tsubota K, Okano H, Oike Y, Ishida S. Angiotensin II type 1 receptor signaling contributes to synaptophysin degradation and neuronal dysfunction in the diabetic retina. Diabetes 2008;57:2191–2198

10. Kowluru RA, Tang J, Kern TS. Abnormalities of retinal metabolism in diabetes and experimental galactosemia. VII. Effect of long-term administration of antioxidants on the development of retinopathy. Diabetes 2001;50:1938–1942

11. Brownlee M. Biochemistry and molecular cell biology of diabetic complications. Nature 2001;414:813–820

12. Kowluru RA, Abbas SN. Diabetes-induced mitochondrial dysfunction in the retina. Invest Ophthalmol Vis Sci 2003;44:5327–5334

13. Boveris A. Mitochondrial production of superoxide radical and hydrogen peroxide. Adv Exp Med Biol 1977;78:67–82

14. Pinto CC, Silva KC, Biswas SK, Martins N, Lopes de Faria JB, Lopes de Faria JM. Arterial hypertension exacerbates oxidative stress in early diabetic retinopathy. Free Radic Res 2007;41:1151–1158

15. Giardino I, Fard AK, Hatchell DL, Brownlee M. Aminoguanidine inhibits reactive oxygen species formation, lipid peroxidation, and oxidant-induced apoptosis. Diabetes 1998;47:1114–1120

16. Mizutani M, Kern TS, Lorenzi M. Accelerated death of retinal microvascular cells in human and experimental diabetic retinopathy. J Clin Invest 1996;97:2883–2890

17. Cogan DG, Toussaint D, Kuwabara T. Retinal vascular patterns. IV. Diabetic retinopathy. Arch Ophthalmol 1961;66:366–378

18. Engerman RL, Kern TS. Retinopathy in animal models of diabetes. Diabetes Metab Rev 1995;11:109–120

19. Bresnick GH, Korth K, Groo A, Palta M. Electroretinographic oscillatory potentials predict progression of diabetic retinopathy: preliminary report. Arch Ophthalmol 1984;102:1307–1311

20. Lopes de Faria JM, Katsumi O, Cagliero E, Nathan D, Hirose T. Neurovisual abnormalities preceding the retinopathy in patients with long-term type 1 diabetes mellitus. Graefes Arch Clin Exp Ophthalmol 2001;239:643–648

21. Carrasco E, Hernández C, Miralles A, Huguet P, Farrés J, Simó R. Lower somatostatin expression is an early event in diabetic retinopathy and is associated with retinal neurodegeneration. Diabetes Care 2007;30:2902–2908

22. Carrasco E, Hernández C, de Torres I, Farrés J, Simó R. Lowered cortistatin expression is an early event in the human diabetic retina and is associated with apoptosis and glial activation. Mol Vis 2008;14:1496–1502

23. Li Y, Zhu H, Kuppusamy P, Roubaud V, Zweier JL, Trush MA. Validation of lucigenin (bis-N-methylacridinium) as a chemilumigenic probe for detecting superoxide anion radical production by enzymatic and cellular systems. J Biol Chem 1998;273:2015–2023

24. Bradford MM. A rapid and sensitive method for the quantification of microgram quantities of protein utilizing the principle of protein dye binding. Anal Biochem 1976;72:248–254

25. Beutler E, Duron O, Kelly BM. Improved method for the determination of blood glutathione. J Lab Clin Med 1963;61:882–888

26. Picaud S, Peichl L, Franceschini N. Dye-induced photolesion in the mammalian retina: glial and neuronal reactions. J Neurosci Res 1993;35:629–642

27. Yang J, Liu X, Bhalla K, Kim CN, Ibrado AM, Cai J, Peng TI, Jones DP, Wang X. Prevention of apoptosis by bcl-2: release of cytochrome c from mitochondria blocked. Science 1997;275:1129–1132

28. Cui Y, Xu X, Bi H, Zhu Q, Wu J, Xia X, Qiushi Ren, Ho PC. Expression modification of uncoupling proteins and MnSOD in retinal endothelial cells and pericytes induced by high glucose: the role of reactive oxygen species in diabetic retinopathy. Exp Eye Res 2006;83:807–816

29. Jung KH, Chu K, Lee ST, Kim SJ, Song EC, Kim EH, Park DK, Sinn DI, Kim JM, Kim M, Roh JK. Blockade of AT1 receptor reduces apoptosis, inflammation, and oxidative stress in normotensive rats with intracerebral hemorrhage. J Pharmacol Exp Ther 2007;322:1051–1058

30. Phipps JA, Wilkinson-Berka JL, Fletcher EL. Retinal dysfunction in diabetic ren-2 rats is ameliorated by treatment with valsartan but not atenolol. Invest Ophthalmol Vis Sci 2007;48:927–934

31. Holopigian K, Greenstein VC, Seiple W, Hood DC, Carr RE. Evidence for photoreceptor changes in patients with diabetic retinopathy. Invest Ophthalmol Vis Sci 1997;38:2355–2365

32. Phipps JA, Fletcher EL, Vingrys AJ. Paired-flash identification of rod and cone dysfunction in the diabetic rat. Invest Ophthalmol Vis Sci 2004;45:4592–4600

33. Yu BP. Cellular defenses against damage from reactive oxygen species. Physiol Rev 1994;74:139–162

34. Kato S, Ishita S, Sugawara K, Mawatari K. Cysteine/glutamate antiporter expression in retinal Müller cells: implications for DL–aminoadipate toxicity. Neuroscience 1993;57:473–482

35. Ewing JF, Maines MD. Glutathione depletion induces heme oxygenase-1 (HSP32) mRNA and protein in rat brain. J Neurochem 1993;60:1512–1519

36. Stocker R, Peterhans E. Antioxidant properties of conjugated bilirubin and biliverdin: biologically relevant scavenging of hypochlorous acid. Free Rad Res Commun 1989;6:57–66

37. Vincent SH. Oxidative effects of heme and porphyrins on proteins and lipids. Semin Hematol 1989;26:105–113

38. Kurihara T, Ozawa Y, Shinoda K, Nagai N, Inoue M, Oike Y, Tsubota K, Ishida S, Okano H. Neuroprotective effects of angiotensin II type 1 receptor (AT1R) blocker, telmisartan, via modulating AT1R and AT2R signaling in retinal inflammation. Invest Ophthalmol Vis Sci 2006;47:5545–5552

39. Sugiyama T, Okuno T, Fukuhara M, Oku H, Ikeda T, Obayashi H, Ohta M, Fukui M, Hasegawa G, Nakamura N. Angiotensin II receptor blocker inhibits abnormal accumulation of advanced glycation end products and retinal damage in a rat model of type 2 diabetes. Exp Eye Res 2007;85:406–412

40. Wilkinson-Berka JL, Tan G, Jaworski K, Ninkovic S. Valsartan but not atenolol improves vascular pathology in diabetic Ren-2 rat retina. Am J Hypertens 2007;20:423–430

41. Matsubara H. Pathological role of angiotensin II type 2 receptor in cardiovascular and renal disease. Circulation 1998;83:1182–1191

42. Imanishi T, Kobayashi K, Kuroi A, Mochizuki S, Goto M, Yoshida K, Akasaka T. Effects of angiotensin II on NO bioavailability evaluated using a catheter-type NO sensor. Hypertension 2006;48:1058–1065

43. Lee CI, Liu X, Zweier JL. Regulation of xanthine oxidase by nitric oxide and peroxynitrite. J Biol Chem 2000;275:9369–9376

44. Nishikawa T, Kukidome D, Sonoda K, Fujisawa K, Matsuhisa T, Motoshima H, Matsumura T, Araki E. Impact of mitochondrial ROS production on diabetic vascular complications. Diabetes Res Clin Pract 2007;77:S41–S45

45. Hoegger MJ, Lieven CJ, Levin LA. Differential production of superoxide by neuronal mitochondria. BMC Neurosci 2008;9:4

46. Sandbach JM, Coscun PE, Grossniklaus HE, Kokoszka JE, Newman NJ, Wallace DC. Ocular pathology in mitochondrial superoxide dismutase (Sod2)-deficient mice. Invest Ophthalmol Vis Sci 2001;42:2173–2178

47. Kowluru RA, Atasi L, Ho YS. Role of mitochondrial superoxide dismutase in the development of diabetic retinopathy. Invest Ophthalmol Vis Sci 2006;47:1594–1599

48. Takahashi A, Masuda A, Sun M, Centonze VE, Herman B. Oxidative stress-induced apoptosis is associated with alterations in mitochondrial caspase activity and Bcl-2-dependent alterations in mitochondrial pH (pHm). Brain Res Bull 2004;62:497–504

49. Kimura S, Zhang GX, Nishiyama A, Shokoji T, Yao L, Fan YY, Rahman M, Abe Y. Mitochondria-derived reactive oxygen species and vascular MAP kinases: comparison of angiotensin II and diazoxide. Hypertension 2005;45:438–444

50. Zhang DX, Chen YF, Campbell WB, Zou AP, Gross GJ, Li PL. Characteristics and superoxide-induced activation of reconstituted myocardial mitochondrial ATP-sensitive potassium channels. Circ Res 2001;89:1177–1183